Dynamics of solitary blood waves in arteries with prostheses

S. Noubissie and P. Woafo
Laboratoire de Mecanique, Faculte des Sciences, Universite de Yaounde I, Boîte Postale 812 Yaounde, Cameroon
(Received 7 February 2001; revised manuscript received 20 September 2002; published 28 April 2003)

We analyze the behavior of blood waves interacting with a prosthesis following the Yomosa nonlinear wave theory extended to include the spatial variation of the arterial radius and wall rigidity. When the prosthesis is short or when its characteristics are close to those of the host artery, the amplitude of the blood solitary wave increases just proximal to the prosthesis and then decreases to a magnitude smaller than the normal value in a healthy vessel. In the presence of an extended prosthesis, we derive the reflection and transmission coefficients at the interfaces, and we thereby obtain the optimal characteristics for an ideal prosthesis. Our results agree qualitatively with known experimental and numerical studies.

DOI: 10.1103/PhysRevE.67.041911 PACS number(s): 87.19.Uv, 87.19.Tt

I. INTRODUCTION

Vascular diseases, in particular those of the arterial type, constitute one of the major causes of mortality in the world. Among these diseases, the most frequent are stenosis, arteriosclerosis, and aneurysm. The major effects of these diseases on blood vessels are the hardening, the softening, the constriction, or the enlargement of the vessel walls. These changes lead to serious circulatory problems with consequences for vital organs, particularly the brain, the heart, and the kidneys [1–3].

When the diseases are still mild, antibiotic treatments sometimes lead to recovery. In severe cases, cardiovascular surgeons remove the damaged area of the vessel. Then they suture the ends of the vessel when the damaged area is not too long or insert a prosthesis if suturing is not possible. In both cases, the mechanical, geometrical, and physical properties of the resulting vessel present an abrupt or a progressive discontinuity. The following questions are therefore interesting. How does the small perturbation of the prosthesis affect the wave pulse? What are the reflection and transmission coefficients for an extended prosthesis? Answers will help to derive the characteristics of an ideal prosthesis allowing pulsatile blood flow without reflection.

To shed some light on these questions, we use the nonlinear wave theory, which, since the pioneering works of Hashimuze [4] and Yomosa [5], has been developed substantially [6–13]. The solitary-wave model gives a plausible explanation for the peaking and steepening of pulsatile waves in arteries.

In Sec. II, we first analyze the flow dynamics interacting with a short prosthesis or a prosthesis with mechanical and geometrical characteristics close to those of the host artery. In Sec. III, we consider an extended prosthesis, derive the coefficients of reflection and transmission, and, from these coefficients, obtain the optimal characteristics of a prosthesis giving perfect transmission at the interfaces. We present our conclusions in Sec. IV.

II. EFFECTS OF PROSTHESES ACTING LIKE SMALL PERTURBATIONS

A. The model

Before analyzing the effects of a prosthesis acting like a small perturbation, we recall some fundamentals of the blood flow in arteries and point out some particular facts related to the soliton theory. We assume the blood to be incompressible and inviscid. The arteries are conical tubes with a nonlinear stress-strain relation. The arterial radius and wall rigidity vary slowly along the tube. The general dynamics describing the blood flow in arteries obeys three laws—the equilibria of momenta and forces, the conservation of mass, and force balance for radial motion of the elastic wall:

$$\frac{\partial v}{\partial t}+\nu\frac{\partial \nu}{\partial z}=-\frac{1}{\rho}\frac{\partial p}{\partial z}, \tag{1a}$$

$$\frac{\partial S}{\partial t}+\frac{\partial(\nu S)}{\partial z}=0, \tag{1b}$$

$$\frac{\rho_0 h}{2\pi R_0}\frac{\partial^2(S-S_0)}{\partial t^2}=p-\frac{h_0 R_0}{R^2}\sigma', \tag{1c}$$

with

$$S-S_0=\pi R^2-\pi R_0^2\approx 2\pi R_0(R-R_0),\quad p=P-P_e,$$

$$\gamma=\frac{(R-R_0)}{R_0},\quad \sigma'=\gamma E(1+a\gamma),$$

where t is the time and z is the coordinate along the propagation axis. The dynamical quantities describing the flow are the longitudinal flow velocity $v(z,t)$, the fluid pressure $P(z,t)$, and the cross-sectional area $S(z,t)$ of the tube (or the radius $R(z,t)$ or the arterial deformation γ). Other parameters are the stress extending in the tangential direction σ', the pressure P_e outside the tube, the density ρ of the fluid, the wall's density ρ_0, Young's modulus E, the equilibrium radius R_0, the nonlinear coefficient of elasticity a, the thickness h contributing to the elastic deformation, and the equilibrium thickness h_0.

In experiments, the equilibrium radius R_0 and Young's modulus E vary along the artery [14]. The radius varies like a decreasing exponential in space ($R_0=R_{00}e^{-mz}$, where m is a positive factor and R_{00} the reference radius) and E follows an increasing exponential law [6–8,14]. Assuming weak exponential laws, the radius is approximately

$$R(z,t)=R_{00}(1-mz)(1+\gamma). \tag{2a}$$

The linear approximation of Young's modulus is

$$E(z)=E_0(1+\lambda z), \tag{2b}$$

with E_0 being a reference value and λ a positive coefficient. For mathematical purposes, we assume that the values of m and λ are small enough and appear at the order $\varepsilon^{5/2}$, where ε is a perturbation parameter. Typical data for the physical and geometrical parameters taken from Ref. [5] for the thoracic aorta are

$$R_{00}=0.5 \text{ cm}, \quad h_0=0.12\ R_{00}, \quad E_0=5.49\times 10^6 \text{ dyn/cm}^2,$$

and for the femoral artery

$$R_{00}=0.15 \text{ cm}, \quad h_0=0.12\ R_{00}, \quad E_{0=14.1}\times 10^6 \text{ dyn/cm}^2,$$

with the following for both:

$$\rho_0=1.05 \text{ g/cm}^3$$

and

$$\rho_0=1.06 \text{ g/cm}^3.$$

The quantities m and λ reported in Refs. [6] and [7] vary from 0.01 to 0.05 cm^{-1} and 0.01 to 0.04 cm^{-1}, respectively.

Let us discuss the limitations and novelties of our model. The two main limitations are the one dimensionality and the inviscid character of the blood. The one dimensionality of the model means that the blood wave components (pressure, velocity, and cross-sectional area) depend only on time and axial coordinate z and not on the transverse and radial coordinates. Moreover, we neglect the transverse components of the velocity. Despite these limitations, this simplified model reproduces many features of natural pulses such as growth and decay of the pulse wave components (see Refs. [4–7]). We also assume that the viscosity effects are negligible. This assumption is only valid for large arteries with a diameter of about 1 cm. However, taking into account viscosity effects modifies the resulting Korteveg–de Vries (KdV) equation by an additive term associated with dissipation [9] and the qualitative effects of the prosthesis will be the same, at least for our simplified model.

The novelties of the model include a nonlinear stress-strain relation that seems to be more realistic than the usual linear elastic relation [5,8]. Unlike other models, which assume the pressure p to be a known function of time (generally sinusoidal), we consider it as a spatiotemporal dynamical quantity to be derived. In fact, when the heart sends an initial blood pulse to the arterial tree, all pulse components, including pressure, vary in time and space as they propagate. A third point is the spatial variation of the radius and Young's modulus as given by Eq. (2), which approximate experimental facts [14].

We first consider the effects of the prosthesis when they weakly perturb the flow dynamics, e.g., when the length of the prosthesis is comparable to that of the pulse wave length or when for a large prosthesis the mismatch between its characteristics and those of the host artery is not large. We thus assume that in the presence of the prosthesis, the radius and the rigidity vary locally by $f_{R,E}(z)$, so that

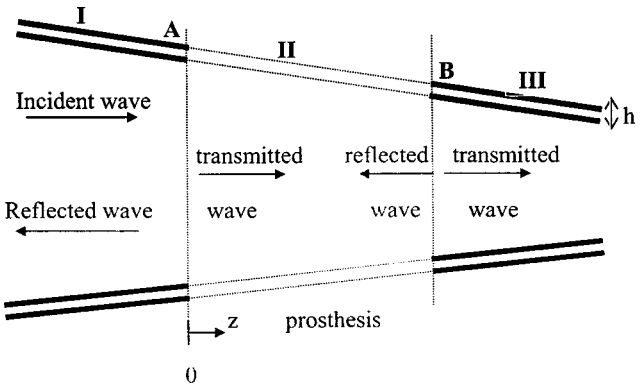

FIG. 1. Geometry of the artery with prosthesis.

$$R(z)=R_{00}[1+\varepsilon^{5/2}F_R(z)+\varepsilon f_R(z)](1+\gamma) \tag{3a}$$

and

$$E(z)=E_0[1+\varepsilon^{5/2}F_E(z)+\varepsilon f_E(z)], \tag{3b}$$

where $F_R(z)=-m'z$ and $F_E(z)=\lambda' z$ (assuming that m and λ have forms $m=\varepsilon^{5/2}m'$ and $\lambda=\varepsilon^{5/2}\lambda'$). Figure 1 shows the geometry of the artery with prosthesis. We define the functions f_R and f_E as

$$f_{R,E}(z)=\alpha_1[\tanh\alpha_2(z-z_{00})-\tanh\alpha_2(z-z_{10})], \tag{4}$$

where α_1 and α_2 measure, respectively, the amplitude and the gradient scales of the perturbation. As α_2 increases, the transition region diminishes, leading to an abrupt perturbation with a rectangular shape. z_{00} and z_{10} are the locations of the sutures at both ends of the prosthesis.

B. Derivation of the perturbed KdV equation

Following the mathematical procedure of Ref. [5], we set

$$\nu'=\varepsilon\nu_1(\xi,\tau)+\varepsilon^2\nu_2(\xi,\tau), \tag{5a}$$

$$p'=\varepsilon p_1(\xi,\tau)+\varepsilon^2 p_2(\xi,\tau), \tag{5b}$$

$$s'=1+\varepsilon s_1(\xi,\tau)+\varepsilon^2 s_2(\xi,\tau), \tag{5c}$$

where $\xi=\varepsilon^{1/2}(z'-t')$ and $\tau=\varepsilon^{3/2}t'$, with the dimensionless quantities

$$\nu=c_0\nu', \quad p=p_0p', \quad t=T_0t', \quad z=L_0z', \quad S=S_0s',$$

$$S_0=\pi R_0^2, \quad c_0=L_0/T_0, \quad L_0=(R_{00}h_0\rho_0/2\rho)^{1/2},$$

$$T_0=(\rho_0R_{00}^2h_0/E_0)^{1/2},$$

and

$$p_0=h_0E_0/2R_{00}.$$

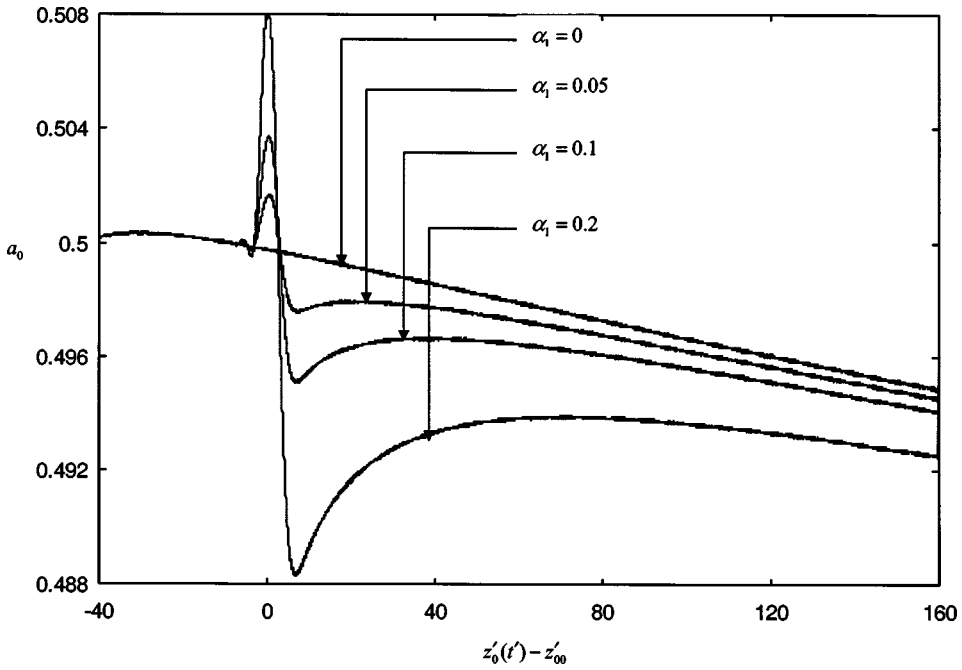

FIG. 2. Spatial variations of the amplitude of the arterial velocity wave for different values of α_1 with $z_{10}'-z_{00}'=5$.

Inserting the transformations (5) into the resulting nondimensional dynamical equations and after some algebraic transformations, we find that the first component v_1 of the velocity wave obeys the following perturbed KdV equation (see the Appendix):

$$\frac{\partial \nu_1}{\partial \tau}+k\nu_1\frac{\partial \nu_1}{\partial \xi}+\frac{1}{2}\frac{\partial^3 \nu_1}{\partial \xi^3}-\frac{1}{2}f_1(\xi,\tau)\frac{\partial \nu_1}{\partial \xi}+\frac{1}{2}f_2(\xi,\tau)\frac{\partial \nu_1}{\partial \xi}=0, \tag{6}$$

with coefficients $k=\frac{1}{2}(a+1)$, $f_1(\xi,\tau)=f_R(\xi,\tau)-m_1'\tau$ and $f_2(\xi,\tau)=f_E(\xi,\tau)+\lambda_1'\tau$.

Using the transformations $\tau=2T$ and $\nu_1=-[6/(a+1)]V_1$, we finally obtain the equation

$$\frac{\partial V_1}{\partial T}-6V_1\frac{\partial V_1}{\partial \xi}+\frac{\partial^3 V_1}{\partial \xi^3}-f_1(\xi,T)\frac{\partial V_1}{\partial \xi}+f_2(\xi,T)\frac{\partial V_1}{\partial \xi}=0. \tag{7}$$

We can derive similar equations for the first components of the dimensionless pressure p_1 and the section s_1 of the arterial wall. Thus the results we obtain below are qualitatively valid for the pressure and wall deformation.

C. Numerical results and comparison

In the absence of the terms $f_1(\xi,\tau)$ and $f_2(\xi,\tau)$, the solution of the KdV equation (7) is

$$V_1=-a_0\,\mathrm{sech}^2[a_0^{1/2}(\xi-4a_0T)], \tag{8}$$

where a_0 is the amplitude of the wave. Equation (8) implies that the blood wave amplitude remains constant during its propagation. In fact, it does not. Experimental measures [1] of the pulse wave changes at five sites of the artery tree of a dog—ascending, thoracic, abdominal, femoral, and saphenous arteries—revealed that the amplitude of the velocity wave v decreases continuously as one moves from the ascending to the saphenous arteries (see, for instance, Fig. 1 of Ref. [5]). This behavior can explain the scattering of blood waves at the arterial branchings, but the spatial variation of the vessel characteristics also plays an important role, as in Fig. 2 (with $\alpha_1=0$).

We integrate the perturbed KdV equation (7) numerically using the finite difference method of Zabusky and Kruskal [15] under periodic conditions with steps $\Delta T=5\times10^{-3}$ and $\Delta\xi=0.1$ over a length $L_\xi=200$.

We launch an initial solitary wave of the unperturbed KdV equation of the form of Eq. (8) at a distance $z'=40$ from the leading edge of the prosthesis, with $a_0=0.5$, $\alpha_2'=\alpha_2L_0=0.045$, $\lambda_1'+m_1'=0.138$, and $\varepsilon=0.2$. The parameters of the thoracic aorta give $a=1.95$. The constraint that our dimensional physical quantities should be as close as possible to those present in living bodies dictates our choice of the values given above (in particular $\lambda_1'+m_1'$, a_0 and ε). Indeed with $a_0=0.5$, a reverse transformation leads to an amplitude $v_{\max}=114$ cm/s for the velocity wave that lies in the range of 80–140 cm/s observed in thoracic and femoral arteries. The corresponding wave width is $L_w=0.39$ cm. Also, from the value of $\lambda_1'+m_1'$, we have $\lambda+m=2m^{-1}$, which is of the same order as the values given before.

Figures 2 and 3 report our numerical results. The horizontal axis is the distance from the center $z_0'(t')$ of the wave to the leading edge z_{00}' of the prosthesis, while the vertical axis corresponds to the maximal amplitude of the wave. Figure 2 presents the effects of the amplitude α_1 of the perturbation $f_{R,E}$ on a_0 as the wave propagates along the artery interacting with the prosthesis ($z_{10}'-z_{00}'=5$ corresponds to $z_{10}-z_{00}=0.615$ cm). For the case $\alpha_1=0$, corresponding to the artery without prosthesis (e.g., a healthy artery), the amplitude of the velocity wave decreases along the artery as mentioned. As α_1 increases, the wave amplitude suffers impor-

tant modifications. As the wave approaches the leading edge of the prosthesis, its amplitude increases progressively to a maximum at the center of the prosthesis. Then it decreases abruptly before trying to recover the value that it would have had in the absence of the prosthesis. Instead, the prosthesis induces a loss of energy to small-amplitude reflected waves generated at the leading edge of the prosthesis. This effect increases as either α_1 or α_2 increases. An increase of the length $(z'_{10}-z'_{00})$ of the prosthesis amplifies the variation of the wave amplitude at the prosthesis site, implying that if a prosthesis replaces an extended segment of the artery, rupture is more probable. If the differences between the properties of the artery and a long prosthesis are large, we must consider the interaction of the wave with the interfaces as in Sec. III.

First, we compare our results to existing data. Figures 2 and 3 are similar to those obtained in the literature. The combined experimental and numerical study of Kim *et al.* [16,17], dealing with blood flow in the vicinity of an end-to-end anastomosis, found that because of the compliance mismatch between the prosthesis and the host artery, the wall shear stress increases just proximal to the anastomosis and then decreases to a magnitude smaller than the normal wall shear stress. Bauernschmitt *et al.* [18] simulated arterial hemodynamics after prosthetic replacement in various parts of the artery tree. They concluded that the replacement increases the pulse pressure and pulse velocity, which corresponds to our findings, since the velocity wave is proportional to pressure wave (see the Appendix). Stergiopulos *et al.* [19] analyzed theoretically and from *in vitro* experiments the interaction of blood waves with an extended arterial stenosis whose shape is similar to the prosthesis presented in this paper. They found that hemodynamically nonsevere and nondetectable stenoses induce wave reflections and that the reflection coefficient increases with the severity of the stenosis. Our Figs. 2 and 3 showing energy loss to reflected waves are compatible with these results even though we treat a prosthesis instead of a stenosis. We also mention the similarity between our results and those of Andersson *et al.* [20] and Tang *et al.* [21] on perturbations of arterial stenoses on blood flow velocity, pressure, and shear stress.

III. REFLECTION AND TRANSMISSION AT THE INTERFACES OF AN EXTENDED PROSTHESIS

When the extent of the prosthesis is large compared to the pulse wavelength, we cannot consider its effects as localized perturbations unless the parameters of the prosthesis are close to those of the artery (the case analyzed in Sec. II). Instead, we treat the situation in which an incoming wave impinges on the first interface of the prosthesis. The transmitted part of the wave continues its motion in a new medium determined by the mechanical and geometrical characteristics of the prosthesis. Afterwards, the wave interacts with the second interface of the prosthesis before entering the natural artery as in Fig. 1 with the prosthesis in region II. The index **i** labels the characteristics and wave components in a region **i** of the structure. For instance, the prosthesis has Young's modulus E_2, stress-strain nonlinear coefficient a_2 (assumed equal to a), wall thickness h_2, and nondimensional wave components v'_2, p'_2, and s'_2. Due to the prosthesis, multiple reflections and transmissions occur so that the wave in each part of the structure consists of various reflected and transmitted waves. We consider only the first interaction of the incident wave at each interface (the incident wave of region II being the wave transmitted at the first interface), assuming that the effects of secondary interactions are negligible. Thus in regions I and II, we assume that we have only one incident wave and one reflected wave while in region III, we have only one transmitted wave.

We use the mathematical procedure of Duan *et al.* [10] for the analysis of reflection and transmission at arterial branchings. In each region **i**, we express the wave components in the form

$$p'_i=\varepsilon p_{i1}+\varepsilon^2 p_{i2}+\cdots,\quad \nu'_i=\varepsilon \nu_{i1}+\varepsilon^2 \nu_{i2},$$

$$s'_i=s_{i0}+\varepsilon s_{i1}+\varepsilon^2 s_{i2}. \tag{9}$$

Since in regions I and II, the wave consists of transmitted (or incident) and reflected waves, we write

$$p_{ij}=p^t_{ij}(\xi,\tau)+p^R_{ij}(\eta,\tau), \tag{10}$$

where the new coordinate η is defined as $\eta=\varepsilon^{1/2}(z'+t')$. Similar expressions are valid for s_{ij} and v_{ij}. Inserting Eqs. (9) and (10) into the flow equations in each region, we find that the incident, reflected, and transmitted waves at different interfaces separating regions I, II, and III are described by the following equations.

Region I:

$$\frac{\partial \nu^i_{11}}{\partial \tau}+\left(\frac{a+1}{2}\right)\nu^i_{11}\frac{\partial \nu^i_{11}}{\partial \xi}+\frac{1}{2}\frac{\partial^3 \nu^i_{11}}{\partial \xi^3}=0, \tag{11a}$$

$$\frac{\partial \nu^R_{11}}{\partial \tau}-\left(\frac{a+1}{2}\right)\nu^R_{11}\frac{\partial \nu^R_{11}}{\partial \eta}+\frac{1}{2}\frac{\partial^3 \nu^R_{11}}{\partial \eta^3}=0, \tag{11b}$$

with $s^i_{11}=p^i_{11}=v^i_{11}$ and $s^R_{11}=p^R_{11}=-v^R_{11}$.

Region II:

$$\frac{\partial \nu^t_{21}}{\partial \tau}+\left(\frac{a+1}{2}\right)\nu^t_{21}\frac{\partial \nu^t_{21}}{\partial \xi}+\frac{1}{2}\frac{\partial^3 \nu^t_{21}}{\partial \xi^3}=0, \tag{11c}$$

$$\frac{\partial \nu^R_{21}}{\partial \tau}-\left(\frac{a+1}{2}\right)\nu^R_{21}\frac{\partial \nu^R_{21}}{\partial \eta}+\frac{1}{2}\frac{\partial^3 \nu^R_{21}}{\partial \eta^3}=0, \tag{11d}$$

with $s^t_{21}=p^t_{21}=\nu^t_{21}$ and $s^R_{21}=p^R_{21}=-\nu^R_{21}$.

Region III:

$$\frac{\partial \nu^t_{31}}{\partial \tau}+\left(\frac{a+1}{2}\right)\nu^t_{31}\frac{\partial \nu^t_{31}}{\partial \xi}+\frac{1}{2}\frac{\partial^3 \nu^t_{31}}{\partial \xi^3}=0, \tag{11e}$$

with $s^t_{31}=p^t_{31}=\nu^t_{31}$. The superscripts *i*, *R* and *t* stand, respectively, for the incident, reflected, and transmitted waves. We note that Eqs. (11) hold only at the interfaces. Far from the interfaces, the waves obey an equation similar to Eq. (6).

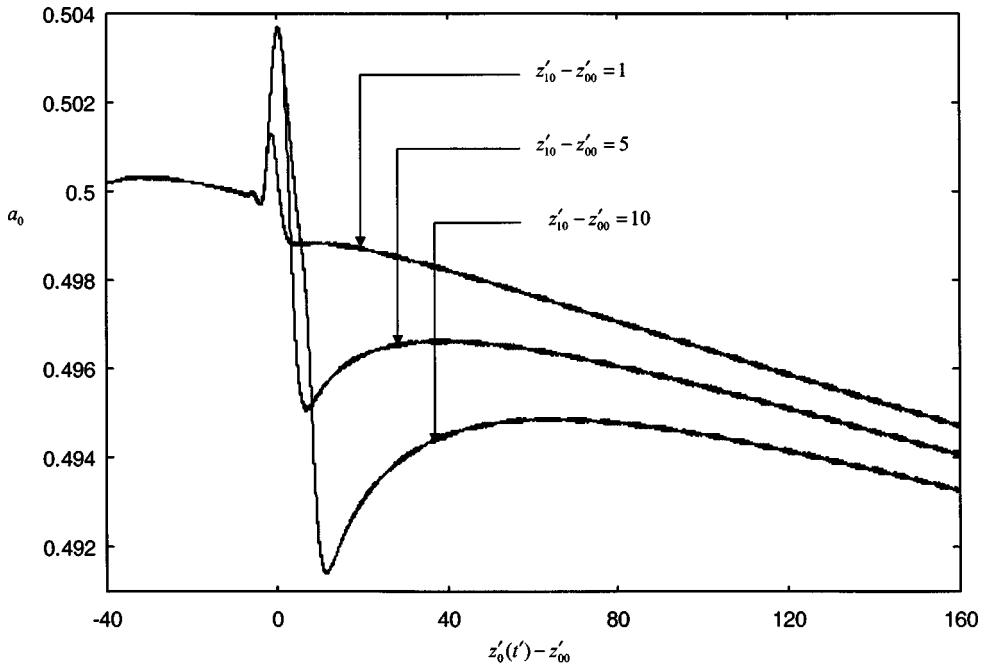

FIG. 3. Effects of the extent of the prosthesis on the spatial variations of the amplitude of the arterial waves with $\alpha_1=0.1$.

To obtain the reflection and transmission coefficients, we use at each interface the continuity of pressure and mass to derive the following.

At the first interface (region I to region II),

$$\frac{E_1h_1}{2R_1}(p_1^i+p_1^R)=\frac{E_2h_2}{2R_2}p_2^t \tag{12a}$$

and

$$(h_1E_1)^{1/2}R_1^{3/2}(\nu_1^i+\nu_1^R)=(h_2E_2)^{1/2}R_2^{3/2}\nu_2^t. \tag{12b}$$

At the second interface (region II to region III),

$$\frac{E_2h_2}{2R_2}(p_2^i+p_2^R)=\frac{E_3h_3}{2R_3}p_3^t \tag{12c}$$

and

$$(h_2E_2)^{1/2}R_2^{3/2}(\nu_2^i+\nu_2^R)=(h_3E_3)^{1/2}R_3^{3/2}\nu_3^t. \tag{12d}$$

From Eqs. (12a) and (12b), the transmitted and reflected pressures related the dimensional incident pressure by the following relations:

$$p_2^t=\frac{2}{1+k_1}p_1^i,\quad p_1^R=\frac{1-k_1}{1+k_1}p_1^i, \tag{13a}$$

with

$$k_1=\left(\frac{R_2}{R_1}\right)^{5/2}\left(\frac{E_1h_1}{E_2h_2}\right)^{1/2}.$$

From Eqs. (12c) and (12d), we can express p_3^t and p_2^R first in terms of p_2^t, then in terms of p_1^i to obtain

$$p_3^t=\frac{4}{(1+k_1)(1+k_2)}p_1^i \tag{13b}$$

and

$$p_2^R=\frac{1-k_2}{1+k_2}\frac{2}{1+k_1}p_1^i, \tag{13c}$$

with

$$k_2=\left(\frac{R_3}{R_2}\right)^{5/2}\left(\frac{E_2h_2}{E_3h_3}\right)^{1/2}.$$

From Eq. (13), we derive two important results for the effects of prostheses on pressure waves. The first result concerns the behavior of the reflection coefficient. The reflection coefficients, which are the ratios p_1^R/p_1^i and p_2^R/p_1^i, depend on the arterial and prosthesis characteristics (radius, Young's modulus, and thickness). Thus we can describe their behavior in terms of the mismatch between the artery and prosthesis. For instance, consider the situation at the entrance of the prosthesis and assume that $h_2=h_1$ and $R_2=R_1$. The effects of the prosthesis are thus due only to the relative value of E_2 compared to E_1. As E_2 increases, the reflection coefficient increases from 0 to 1. This behavior is also compatible with the effects of the severity of an extended stenosis as obtained by Stergiopulos *et al.* [19].

Our second and most interesting result is that, from the expressions for p_1^R and p_2^R, we derive the constraints on the prosthesis and artery that eliminate reflections at the interfaces. Setting $p_1^R=p_2^R=0$, we obtain the relations

$$\left(\frac{R_1}{R_2}\right)^{5/2}\left(\frac{E_2h_2}{E_1h_1}\right)^{1/2}=1, \tag{14a}$$

and

$$\left(\frac{R_2}{R_3}\right)^{5/2}\left(\frac{E_3h_3}{E_2h_2}\right)^{1/2}=1. \tag{14b}$$

Equation (14) gives what we call the optimal shape for an extended prosthesis that suppresses reflection of waves at its interfaces. Since the mechanical properties (for instance, Young's modulus E_2) of the prosthesis are difficult to adjust, we take E_2 as given and vary the geometrical characteristics R_2 and h_2 at the first interface to satisfy Eq. (14a) and at the second interface according to Eq. (14b). If we assume that the characteristics of the arteries in regions I and II are the same (such as when the artery radius and modulus do not vary along the artery axis), then Eqs. (14a) and (14b) are equivalent and the optimal thickness of the prosthesis is

$$h_2=\left(\frac{R_2}{R_1}\right)^5\frac{E_1h_1}{E_2}, \tag{15}$$

which is inversely proportional to Young's modulus of the prosthesis material. Assuming that $R_2=R_1$, and using the data given in Sec. II, we obtain that in the thoracic aorta, the optimal prosthesis thickness is $h_2=3.294\times10^5/E_2$ cm, while in the femoral artery, $h_2=2.538\times10^5/E_2$ cm with the prosthesis of Young's modulus E_2 (which depends on the polymeric material used) given in dyn/cm^2.

However, if the characteristics of the artery vary along its axis, then the prosthesis should have a conical shape whose span agrees with both Eq. (14). If the radius R_2 is chosen to be equal to R_1 at the entrance and to R_3 at the exit of the prosthesis, the ratio R_a between the thicknesses at the entrance and at the exit of the prosthesis should be

$$R_a=\frac{1+\lambda z_{\mathrm{en}}}{1+\lambda z_{\mathrm{ou}}}, \tag{16}$$

where z_{en} and z_{ou} are, respectively, the coordinates of the entrance and exit of the prosthesis.

IV. CONCLUSION

This paper treats the interactions of blood waves with prostheses. For short prostheses or prostheses with characteristics nearly equal to those of the host artery, the blood wave obeys a perturbed KdV equation. The numerical simulation of this equation shows amplitude variation consisting of an increase just proximal to the prosthesis, followed by an abrupt decrease, and then an increase leading to an amplitude smaller than the normal value of a healthy vessel. Our results are qualitatively similar to those obtained from experimental studies and other numerical simulations of blood flow in arteries with prostheses and stenoses. The main consequence of the increase and decrease of the amplitude of each pulse wave at the prosthesis is to induce abnormal stress on the arterial and prosthesis walls, one of the main causes of prosthesis failure or rupture. An extended prosthesis scatters KdV solitons into reflected and transmitted solitons at each interface. The coefficients of reflection and transmission depend on the mechanical and geometrical characteristics of the prosthesis and artery. We have derived the relation between the prosthesis and artery characteristics, which eliminates the reflections at both interfaces, thus defining an ideal prosthesis.

An interesting question, which remains unsolved, is the case of an abrupt change in arterial wall parameters. In this case, we could solve the generating Euler equations (1) analytically as in the study of the interactions of water waves with variable channel bottoms [22,23] or numerically by the generalized finite difference method introduced in Ref. [21].

ACKNOWLEDGMENTS

The authors thank Professors K. B. Chandran (Biomedical Engineering, The University of Iowa, U.S.) and H.I. Andersson (Dept. of Applied Mechanics, NTNU, Norway) for providing assistance.

APPENDIX

Let us rewrite the set of equations (1),

$$\frac{\partial\nu}{\partial t}+\nu\frac{\partial\nu}{\partial z}=-\frac{1}{\rho}\frac{\partial p}{\partial z},$$

$$\frac{\partial S}{\partial t}+\frac{\partial(\nu S)}{\partial z}=0, \tag{A1}$$

$$\frac{\rho_0 h}{2\pi R_0}\frac{\partial^2(S-S_0)}{\partial t^2}=p-\frac{h_0R_0}{R^2}\gamma E(1+\alpha\gamma),$$

$$\text{with}\quad \gamma=\frac{R-R_0}{R_0}=\frac{S-S_0}{2S_0}.$$

The condition for the conservation of mass of the wall and tissue (see Ref. [5]) leads to

$$R_0h_0=Rh.$$

Then, using relations (3a) and (3b), we can write

$$R=R_{00}(1+p_R)(1+\gamma)$$

and

$$E=E_0(1+p_E),$$

where

$$p_{R,E}=\varepsilon^{5/2}F_{R,E}(z)+\varepsilon f_{R,E}(z).$$

Using the dimensionless quantities defined in Eqs. (5), the system (A1) becomes

$$\frac{\partial\nu'}{\partial t'}+\nu'\frac{\partial\nu'}{\partial z'}+\frac{\partial p'}{\partial z'}=0,$$

$$(1+p_R)\frac{\partial s'}{\partial t'}+2s'\nu'\frac{\partial p_R}{\partial z}+(1+p_R)\nu'\frac{\partial s'}{\partial z'}+(1+p_R)s'\frac{\partial \nu'}{\partial z'}=0,$$

$$(1+p_R)^2(1+s')\frac{\partial^2 s'}{\partial t'^2}=\tfrac{1}{2}(1+p_R)p'(1+s')^2-(1+p_E)(s'-1)(2+as'-a). \tag{A2}$$

Inserting the scale transformation $\xi=\varepsilon^{1/2}(z'-t')$ and $\tau=\varepsilon^{3/2}t'$ into (A2), we obtain

$$-\frac{\partial \nu'}{\partial \xi}+\varepsilon\frac{\partial \nu'}{\partial \tau}+\nu'\frac{\partial \nu'}{\partial \xi}+\frac{\partial p'}{\partial \xi}=0,$$

$$[1+\varepsilon f_R-m_1'(\xi\varepsilon^2+\tau\varepsilon)]\left(-\frac{\partial s'}{\partial \xi}+\varepsilon\frac{\partial s'}{\partial \tau}\right)+2s'\nu'\times\varepsilon^{1/2}\left(\frac{\partial f_R}{\partial \xi}-m_1'\varepsilon^{3/2}\right)+[1+\varepsilon f_R-m_1'(\xi\varepsilon^2+\tau\varepsilon)]\nu'\frac{\partial s'}{\partial \xi}+[1+\varepsilon f_R-m_1'(\xi\varepsilon^2+\tau\varepsilon)]s'\frac{\partial \nu'}{\partial \xi}=0, \tag{A3}$$

$$[1+\varepsilon f_R-m_1'(\xi\varepsilon^2+\tau\varepsilon)]^2(1+s')\times\left(\varepsilon\frac{\partial}{\partial \xi^2}-2\varepsilon^2\frac{\partial^2}{\partial \xi\partial \tau}+\varepsilon^3\frac{\partial^2}{\partial \tau^2}\right)s'=\tfrac{1}{2}[1+\varepsilon f_R-m_1'(\xi\varepsilon^2+\varepsilon\tau)](1+s')^2p'-[1+\varepsilon f_E+\lambda_1'(\xi\varepsilon^2+\varepsilon\tau)](s'-1)(2-as'-a),$$

where $m_1'=m'L_0$ and $\lambda_1'=\lambda' L_0$.

We then introduce the perturbation expansions of v', p' and s' [see Eqs. (5)] in (A3) and keeping only terms that are, respectively, proportional to ε and ε^2, we obtain for ε^1,

$$-\frac{\partial \nu_1}{\partial \xi}+\frac{\partial p_1}{\partial \xi}=0, \tag{A4a}$$

$$-\frac{\partial s_1}{\partial \xi}+\frac{\partial \nu_1}{\partial \xi}=0, \tag{A4b}$$

$$2p_1-2s_1=0, \tag{A4c}$$

and for ε^2,

$$-\frac{\partial \nu_2}{\partial \xi}+\frac{\partial \nu_1}{\partial \tau}+\nu_1\frac{\partial \nu_1}{\partial \xi}+\frac{\partial p_2}{\partial \xi}=0, \tag{A5a}$$

$$-\frac{\partial s_2}{\partial \xi}+\frac{\partial s_1}{\partial \tau}+(f_R-m_1'\tau)\left(-\frac{\partial s_1}{\partial \xi}\right)+\nu_1\frac{\partial s_1}{\partial \xi}+\frac{\partial \nu_2}{\partial \xi}+s_1\frac{\partial \nu_1}{\partial \xi}+(f_R-m_1'\tau)\left(-\frac{\partial s_1}{\partial \xi}\right), \tag{A5b}$$

$$2\frac{\partial^2 s_1}{\partial \xi^2}=\tfrac{1}{2}[4p_2+4s_1p_1+4(f_R-m_1'\tau)p_1]-as_1^2-(f_E-\lambda_1'\tau)s_1^2-2s_2. \tag{A5c}$$

Combining Eqs. (A4) we obtain

$$p_1=s_1=\nu_1.$$

From Eq. (A5c), we have

$$p_2=\frac{\partial^2 s_1}{\partial \xi^2}-s_1p_1-p_1(f_R-m_1'\tau)+\tfrac{1}{2}as_1^2+s_1(f_E-\lambda_1'\tau)+s_2.$$

Substituting this relation into Eqs. (A5a) and (A5b) leads to

$$\frac{\partial \nu_2}{\partial \xi}-\frac{\partial s_2}{\partial \xi}=g_1,$$

$$-\frac{\partial \nu_2}{\partial \xi}+\frac{\partial s_2}{\partial \xi}=g_2, \tag{A6}$$

with

$$g_1=\frac{\partial \nu_1}{\partial \tau}+\nu_1\frac{\partial \nu_1}{\partial \xi}+\frac{\partial^3 s_1}{\partial \xi^3}-\frac{\partial s_1^2}{\partial \xi}-(f_R-m_1'\tau)\frac{\partial s_1^2}{\partial \xi}+\frac{a}{2}\frac{\partial s_1^2}{\partial \xi}+(f_E-\lambda_1'\tau)\frac{\partial s_1}{\partial \xi},$$

$$g_2=\frac{\partial s_1}{\partial \tau}-(f_R-m_1'\tau)\frac{\partial s_1}{\partial \xi}+\nu_1\frac{\partial s_1}{\partial \xi}+s_1\frac{\partial \nu_1}{\partial \xi}+\frac{a}{2}\frac{\partial s_1^2}{\partial \xi}+(f_R-m_1'\tau)\frac{\partial \nu_1}{\partial \xi}.$$

This result implies

$$g_1+g_2=0,$$

and finally, the equation,

$$\frac{\partial \nu_1}{\partial \tau}+\frac{1}{2}(a+1)\nu_1\frac{\partial \nu_1}{\partial \xi}+\frac{1}{2}\frac{\partial^3 \nu_1}{\partial \xi^3}+\frac{1}{2}[f_E-f_R+(m_1'+\lambda_1')\tau]\frac{\partial \nu_1}{\partial \xi}=0.$$

Setting $k=\frac{1}{2}(a+1)$, $f_1=f_R-m_1'\tau$, $f_2=f_E+\lambda_1'$, τ, we obtain

$$\frac{\partial \nu_1}{\partial \tau}+k\nu_1\frac{\partial \nu_1}{\partial \xi}+\frac{1}{2}\frac{\partial^3 \nu_1}{\partial \xi^3}-\frac{1}{2}f_1(\xi,\tau)\frac{\partial \nu_1}{\partial \xi}+\frac{1}{2}f_2(\xi,\tau)\frac{\partial \nu_1}{\partial \xi}=0,$$

which is Eq. (6) in the text.

[1] D. A. McDonald, J. Biomech. **12**, 13 (1979); D. A. McDonald, *Blood Flow in Arteries*, 2nd ed. (Edward Arnold, London, 1974).
[2] D. F. Young, J. Biomech. Eng. **101**, 157 (1979).
[3] J. C. Misra, M. K. Patra, and S. C. Misra, J. Biomech. **26**, 1129 (1993).
[4] Y. Hashimuze, J. Phys. Soc. Jpn. **54**, 3305 (1985); **57**, 4160 (1988).
[5] S. Yomosa, J. Phys. Soc. Jpn. **56**, 506 (1987).
[6] J. F. Paquerot and S. G. Lambrakos, Phys. Rev. E **49**, 3432 (1994).
[7] J. F. Paquerot and M. Remoissenet, Phys. Lett. A **194**, 77 (1994).
[8] A. Sakanishi, M. Hasegawa, and Y. Ushiyama, Phys. Lett. A **221**, 395 (1996).
[9] W.-S. Duan, B.-R. Wang, and R.-J. Wein, J. Phys. Soc. Jpn. **65**, 945 (1996).
[10] W.-S. Duan, B.-R. Wang, and R.-J. Wein, Phys. Rev. E **55**, 1773 (1997).
[11] H. Demiray, Int. J. Nonlin. Mech. **33**, 363 (1998).
[12] W. Malfliet and I. Ndayirinde, Physica D **123**, 92 (1998).
[13] G. Akgun and H. Demiray, Int. J. Nonlin. Mech. **34**, 571 (1999); **35**, 597 (2000).
[14] Y. C. Fung, *Biomechanics* (Springer, Berlin, 1994); D. J. Patel, F. M. De Freitas, J. C. Greenfield, and D. L. Fry, J. Appl. Physiol. **18**, 1111 (1963).
[15] N. J. Zabusky and M. D. Kruskal, Phys. Rev. Lett. **15**, 240 (1965).
[16] Y. H. Kim, K. B. Chandran, T. J. Bower, and J. D. Corson, Ann. Biomed. Eng. **21**, 311 (1993).
[17] Y. H. Kim and K. B. Chandran, Biorheology **30**, 117 (1993).
[18] R. Bauernschmitt, S. Schultz, A. Schwarzhaupt, U. Kiencke, C.-F. Vahl, R. Lange, and S. Hagl, Ann. Thorac. Surg. **67**, 676 (1999).
[19] N. Stergiopulos, M. Spiridon, F. Pythoud, and J.-J. Meister, J. Biomech. **29**, 31 (1996).
[20] H. I. Andersson, R. Halden, and T. Glomsaker, J. Biomech. **33**, 1257 (2000).
[21] D. Tang, C. Yang, and D. N. Ku, Comput. Struct. **72**, 357 (1999); D. Tang, C. Yang, S. Kobayashi, and D. N. Ku, Appl. Numer. Math. **36**, 299 (2001).
[22] R. Camassa and Y. Y.-T. Wu, Physica D **51**, 295 (1991).
[23] N. Sugimoto, N. Nakajima, and T. Kakutani, J. Phys. Soc. Jpn. **56**, 1717 (1987).